BNL-98926-2012-TECH
C-A/AP/472;BNL-98926-2012-IR

Improvement of the Q-factor measurement in RF cavities

W. Xu

November 2012

Collider Accelerator Department
Brookhaven National Laboratory

U.S. Department of Energy
USDOE Office of Science (SC)

DISCLAIMER

BNL-98926-2012-IR

C-A/AP/#472
November 2012

Improvement of the Q-factor measurement in RF cavities

**Wencan Xu, S. Belomestnykh,
I. Ben-Zvi, H. Hahn**

**Collider-Accelerator Department
Brookhaven National Laboratory
Upton, NY 11973**

Improvement of the Q-factor measurement in RF cavities

Wencan Xu[#,1], S. Belomestnykh[1,2], I. Ben-Zvi[1,2], H. Hahn[1]

[1)] Collider-Accelerator Department, Brookhaven National Lab, Upton, NY 11973, USA
[2)] Physics & Astronomy Department, Stony Brook University, Stony Brook, NY 11794, USA

Abstract

The *Q* values of Higher-order-modes (HOMs) in RF cavities are measured at room temperature with the 3 dB bandwidth reading by a network analyzer. The resonant curve distortion is created by the resonance splitting due to the ellipticity caused by manufacture tolerance and RF ports. Therefore, the measured *Q* values are usually lower than the simulated or theoretical *Q* values. In some cases, even only one mode's *Q* can be measured with the 3 dB method. There may be two reasons for this happening. One is that only one mode was excited and the neighbor splitmode was close to 90º polarized; the other reason is that the resonant curve of one mode was distorted by the other mode too much to measure the 3dB range. In this paper, we resolve this issue by looking into the RF measurement setup, including cavity, input coupler and pick-up coupler, from the equivalent circuit and wave point of view. Based on the BNL3 copper prototype cavity, we compared these results from measurement and simulation.

I. INTRODUCTION

In room temperature higher-order-mode (HOM) measurements, the *Q* values of the HOMs are measured with the 3 dB bandwidth reading at a network analyzer, which excites and picks up RF signal through the fundamental power coupler (FPC) port on one side of the the cavity and pick-up port on the other side of the cavity. This is a good and simple method as long as there is no overlap of the two modes' resonant curves, which means that the frequencies of the two neighbor modes are separated far enough.

However, due to the manufacture tolerance, FPC port and pick-up port make the cavity elliptical, which results in the polarization of the higher order polarized modes, like dipole modes. Therefore, the same type of dipole mode will split into two polarized modes with very-close frequencies, which should have similar *Q* values, theoretically or in simulation. But the readout in the network analyzer is the result of adding up the two modes (magnitude and phase), which makes the 3 dB bandwidths of the two modes to be distorted. Additionally, one mode usually has a stronger coupling than the other due to the location of the RF ports. As a consequence of that, the *Q* values by 3 dB bandwidth are no longer accurate. So, in this paper, we explained the *Q* distortion firstly, and improved the measurement results of *Q* values based on the BNL3 copper prototype cavity, which was designed for a high current SRF linac [1].

This paper is organized as follows. Section II addresses the measurement results of the first 20 dipole modes (10 types HOM) in the BNL3 cavity and compares them to the results from the 3D code Omega3P [2]. Section III explains the mode splitting, the RF measurement setup from both equivalent circuit and electromagnetic field point of view, and derives the S_{21} formula with two splitting modes. Section IV will use the S_{21} formula to fit the measurement S_{21} data and get new *Q* values, and compare the fitting results with measured and simulated Q values. The paper concludes with a short summary of the measurement setup, models and comparison of the results.

[#]wxu@bnl.gov

II. BNL3 CAVITY MEASUREMENT SETUP AND RESULTS

The measureent setup for BNL3 copper prototype cavity is shown in Fig. 1. The BNL3 cavity has one FPC port at one side and one pickup port at the other side of the cavity. In RF superconducting accelerators, the fundamental power coupler (FPC) port is used to deliver high RF power from RF sources to the cavity and the pickup is used to pick up little RF signal in the cavity to measure and control the RF field in the cavity. However, in the warm RF measurement for the copper prototype, either FPC port or pickup port can be used for RF input port or pickup port, and both of them will be made as weak coupling as possible. We used this prototype to study the HOM damping performance of the cavity design. For this paper's study, Fig. 2 shows the first dipole passband's spectrum taken by the network analyzer. It shows that every dipole mode splits into two modes and their resonant curves are distorted by each other.

FIG. 1: Setup of the measurement with closed beam pipe

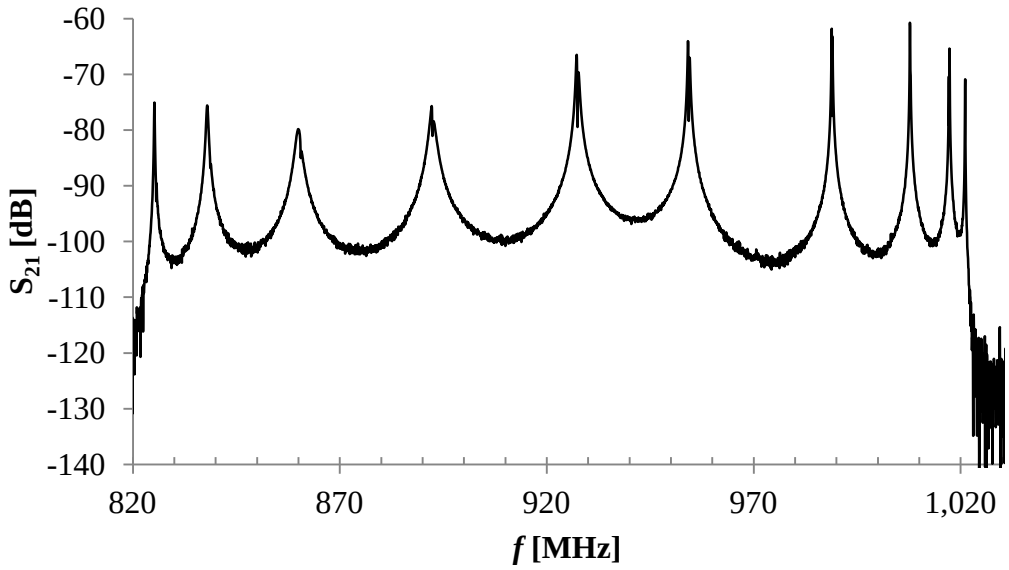

FIG. 2: First dipole mode passband with closed beam pipe

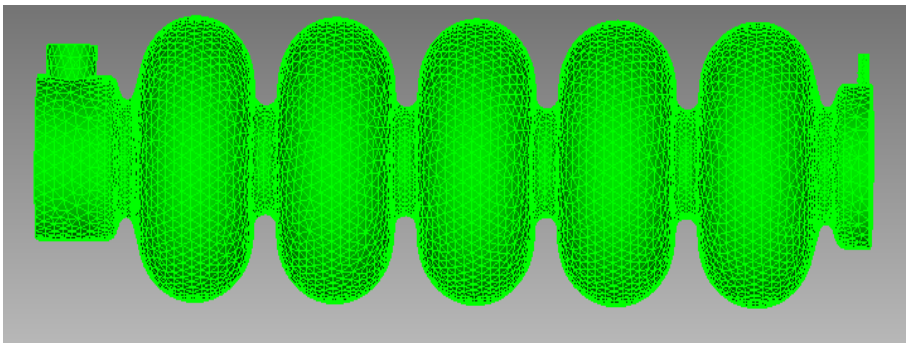

FIG. 3: Simulation model for the Setup of the measurement with closed beam pipe

A 3D cavity model with FPC port and PU port was built for the HOM study, as it is shown in Fig. 3. The comparison of simulation and measurement results of the first dipole passband is shown in Fig. 4. First of all, it shows that the simulated *Q* values are higher than the measured *Q* values. Secondly, most of the modes come as a pair of split modes, which is because of polarization of the dipole modes. In the next section, we will explain these two phenomena.

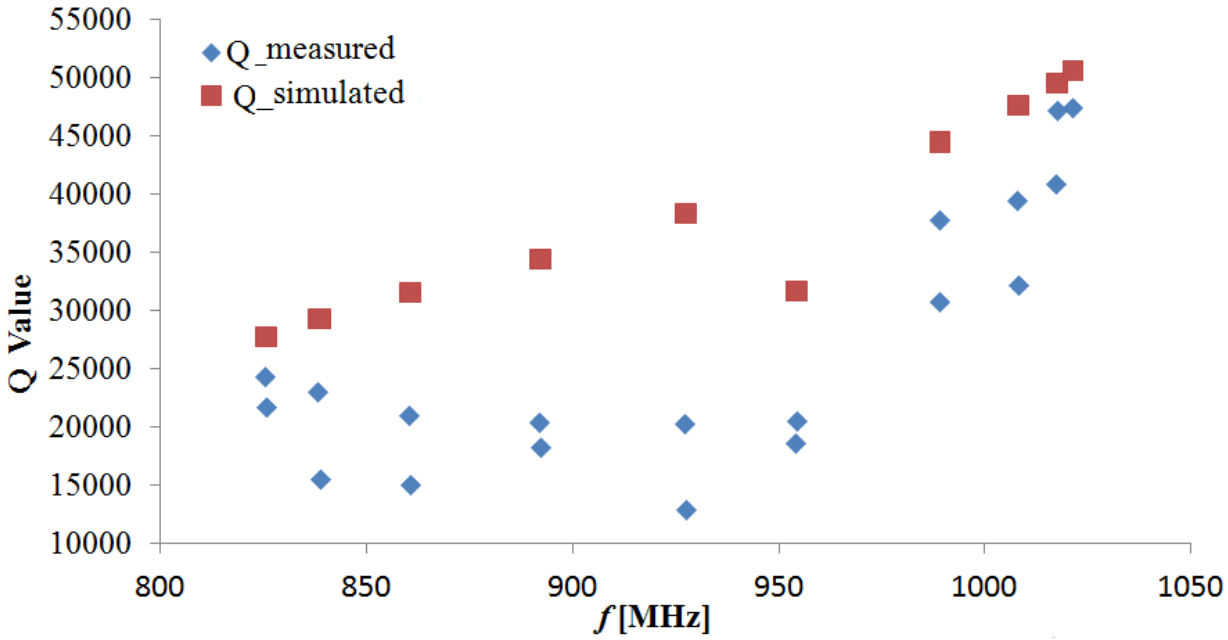

FIG 4: Comparison results from measurement and simulations of BNL3 cavity

III. EXPLANATION OF THE Q-DEDUCTION

3.1 The modes' splitting in RF cavity

Due to manufacture tolerances and manufacture errors, the shape of the circular cross section of the cavity usually is distorted and even the beam pipe is imperfectly cylindrical, causing the cross section of the cavity to be slightly elliptical. Additionally, RF ports (FPC, pick-up and HOM couplers) on the cavity also produce polarization of the cavity. The important consequence of the imperfection and polarization is to split an original mode into two components in line. A simple model to explain the mode splitting is to look into the modes in elliptical waveguide, where odd mode and even mode always exist due to the polarized cross section, as it is shown in

Fig. 5. Fig. 5 (left) shows the split modes in an elliptical waveguide and the total field by adding up the two modes in Fig. 5 (right). As far as the cavity is concerned, a dipole mode will split into two modes with close frequencies and similar *Q* values. Additionally, because of the close frequency and similar *Q* value of the two modes, the network analyzer sees the overlap of these two modes, a typical example of this phenomena measured in BNL3 copper prototype is shown in Fig. 6. It shows that both modes are distorted by each other, and actually the bandwidth of the resonant curve is broadened, so that the measured Q values are usually lower than what it should be. Additionally, the coupling factors of the two modes usually are different from each other, so the nominal field amplitudes of the two modes are different. This will cause one S_{21} curve is distorted more than the other mode.

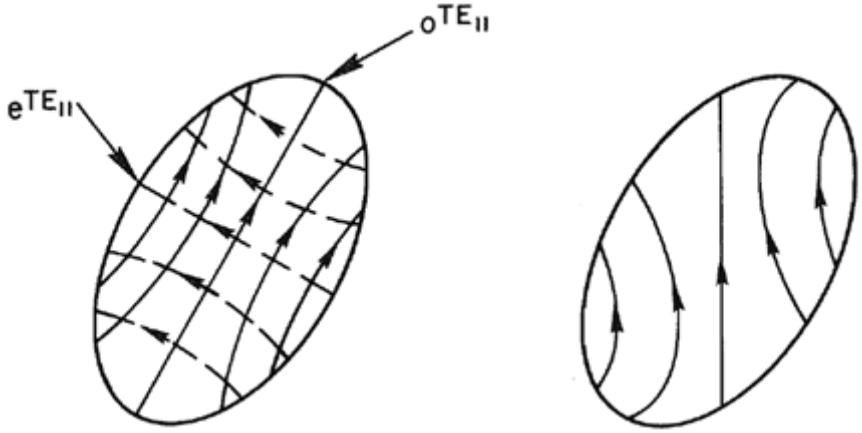

FIG. 5: Left: two splitting modes in the elliptical waveguide; Right: the total field profile

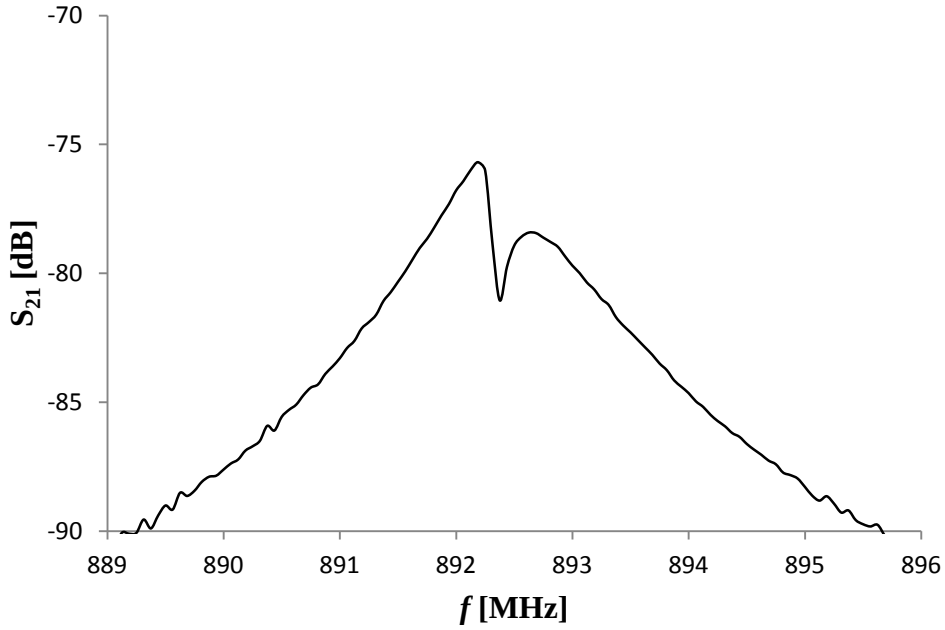

FIG. 6: Typical S_{21} curve of the splitting modes

The theoretical solutions for modes in an elliptical waveguide have been studied and published in references [3, 4]. The field in the elliptical waveguide was solved by using elliptical coordinates, and Maxwell's equations can be separated into Mathieu equations. And then, the resonant frequency of an elliptical waveguide was given by [5]:

$$f^{o,e} = \frac{c}{\pi\rho}\sqrt{q^{o,e}} \qquad (1)$$

Where $f^{o,e}$ is the odd and even mode's frequency; a is the physical semi-major axis of the elliptical waveguide and ρ is the focal distance of the ellipse. The a and ρ defined the eccentricity ε of the waveguide: $\varepsilon = \rho / a$. The values of Mathieu function $q^{o,e}$ for a given mode are rather complicated and reference [5] gave these values for different modes. Electromagnetic fields are treated with Mathieu functions but due to their unfamiliarity are replaced here by a qualitatively correct illustration for the dipole mode in the typical case of $\varepsilon \ll 1$ and the parameter $q \approx \varepsilon$. The fields on the wall boundary of an elliptical pill box cavity, that are relevant to the S_{21} transmission measurements, are approximated by an even and an odd function, [6]

$$u_e \propto \frac{J_1(2\sqrt{q}/\varepsilon)}{\sqrt{1-q^2\cos^2(\eta-\psi)}}\left[\cos(\eta-\psi)-(q/8)\cos 3(\eta-\psi)+...\right] \qquad (1)$$

and $$u_o \propto \frac{J_1(2\sqrt{q}/\varepsilon)}{\sqrt{1-q^2\cos^2(\eta-\psi)}}\left[\sin(\eta-\psi)-(q/8)\sin 3(\eta-\psi)+...\right] \qquad (2)$$

where η is the angular probe position and ψ the excitation angle versus the major axis. The approximated *q*-parameter depends on ε and is defined via the perfect cutoff frequency as $2\sqrt{q}/\varepsilon = j'_{11}$, solution of the Bessel function, $J'_1(j'_{11}) = 0$. In contrast to the minimal effect of eccentricity on field shape, the cut-off frequencies are noticeably split into even and odd solutions with their values changed as

$$f = f_{CO}E[\varepsilon^2]2/\pi \approx f_{CO}\left(1 \pm \frac{\varepsilon}{4} \pm \frac{3\varepsilon^2}{64} + ...\right) \qquad (3)$$

where $E(\varepsilon^2)$ is the complete elliptical integral of the second kind and the $\pm$ serves for the even (-) and odd (+) functions. The measured frequency deviations of $\Delta = \pm 4.2\times10^{-4}$ yield the numerical $\varepsilon = 0.00105$ and the focal distance $h = \varepsilon a \approx 0.21$ mm .

3.2 Measurement model and Equivalent circuit point of view

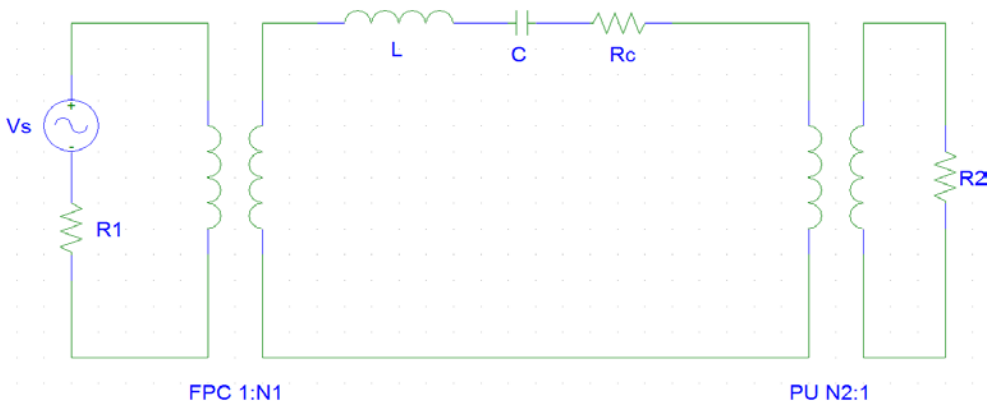

FIG. 7: Equivalent model of the

The measurement setup in Fig. 1 can be modeled as a lumped circuit in Fig. 7, where the cavity and couplers are represented by a RLC circuit and two transformers, respectively. First of all, we assumed only one mode is excited and picked up, so under steady state condition, the S_{21} that is seen by network analyzer can be written as

$$S_{21}(\omega,\omega_0,\beta_e,\beta_t,Q_0)=\frac{2\beta_e\cdot\beta_t}{\left\{1+\beta_e+\beta_t+jQ_0(\frac{\omega}{\omega_0}-\frac{\omega_0}{\omega})\right\}}=\left|S_{21}(\omega_0)\right|e^{j\Phi_0} \qquad (5)$$

Where, ω is frequency, ω_0 is the resonant frequency of the cavity and Q_0 is the unload quality factor of the cavity. The coupling factor of the input coupler is $\beta_e=\frac{Q_0}{Q_e}=\frac{N1^2R_1}{R_c}$ and the coupling factor of pick-up signal is $\beta_t=\frac{Q_0}{Q_t}=\frac{N2^2R_2}{R_c}$. In the test, the loaded Q values $Q_L=Q_0/(1+\beta_c+\beta_t)$ so the S_{21} expression can be re-written as follows .

$$S_{21}(\omega_0,\omega,\beta_e,\beta_t,Q_L)=\sqrt{\frac{4\beta_e\cdot\beta_t}{[1+Q_L{}^2(\frac{\omega}{\omega_0}-\frac{\omega_0}{\omega})^2]}}\cdot(1-jQ_L(\frac{\omega}{\omega_0}-\frac{\omega_0}{\omega})) \qquad (6)$$

3.3 Wave point of view: single mode

Although a lumped circuit is clearly enough to understand the measurement setup, it can also be explained from the electromagnetic field point of view. In this case, a cavity with external excitation $E_0e^{j\omega t}$ input can be represented by a damping differential equation.

$$\frac{d^2E}{dt^2}+\omega_0^2E+\frac{\omega_0}{Q_L}\frac{dE}{dt}=\kappa_{FPC}E_0e^{j\omega t} \qquad (7)$$

Where, under the extremely weak coupling condition, ω_0 is the cavity intrinsic resonant frequency, $Q_L = Q_0$ is the intrinsic *Q* factor of the cavity. The trial solution of this differential equation for the field amplitude in the cavity is $E = Ae^{i\omega t}$, and

$$A = \frac{\kappa_{FPC} E_0}{(\omega_0^2 - \omega^2) + j\frac{\omega\omega_0}{Q_L}} \qquad (8)$$

Where, κ is a constant, which depends on the coupling to the input field. When the input frequency is close to the intrinsic frequency of the cavity, the pickup signal from the probe is proportional to the field in the cavity, so the ratio of pickup field to the exciting field can be written as

$$R = \frac{\kappa_{PU}\kappa_{FPC} E_0}{(\omega_0^2 - \omega^2) + j\frac{\omega\omega_0}{Q_L}} \qquad (9)$$

The formula (6) corresponds to the S_{21} that is the output from the network analyzer. Then, we can get a similar S_{21} formula but from field solution.

$$S_{21}(\omega, \omega_0, Q_0, K) = \frac{K}{\sqrt{[Q_0(\frac{\omega_0}{\omega} - \frac{\omega}{\omega_0})]^2 + 1}} \arg[Q_0(\frac{\omega_0}{\omega} - \frac{\omega}{\omega_0}) + j] \qquad (10)$$

Where, K is a constant dependent on the coupling factors and the *Q*-value. Comparing formula (6) and (10 , the generic transmission coefficient of a single resonance $S_{21}(\omega, \omega_0, Q_0, D)$ can be rewritten as

$$S_{21}(\omega, \omega_0, Q_0, D) = \frac{D}{\sqrt{1 + [Q_0(\frac{\omega_0}{\omega} - \frac{\omega}{\omega_0})]^2}} e^{j\Phi} \qquad (11)$$

Where, D is another constant related to the coupling of FPC and PU and Φ the phase shift against the driving signal.

3.4 The S21 of two close frequencies' modes.

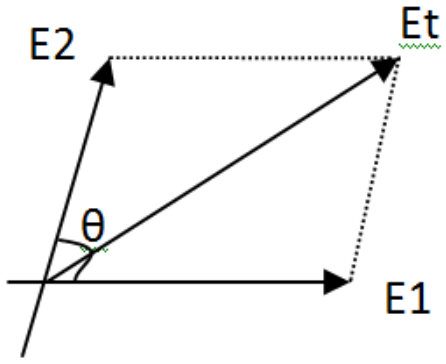

FIG. 8: Sum of phasors of two modes' field

The above S21 formulas are gotten by assuming that only one mode exists in the cavity. However, in the realistic measurement, the S21 curve will be distorted due to the reasons explained above. The excitation signal is common to both split modes, and the S_{21} measured by network analyzer is the sum of two RF waves.

As it is shown in Fig.8, if the angle between two fields is $\theta = \Phi_1 - \Phi_2$, then the new S_{21} contained two modes is

$$S_{21} = \sqrt{\left|S_{21}(\omega_1)\right|^2 + \left|S_{21}(\omega_2)\right|^2 + 2S_{21}(\omega_1)S_{21}(\omega_2)\cos(\Phi_2 - \Phi_1)} \qquad (12)$$

and explicitely

$$S21_{total} = \sqrt{\frac{D_1^2}{1+[Q_{01}(\frac{\omega_{01}}{\omega}-\frac{\omega}{\omega_{01}})]^2} + \frac{D_2^2}{1+[Q_{02}(\frac{\omega_{02}}{\omega}-\frac{\omega}{\omega_{02}})]^2} - \frac{2D_1D_2\cos(\pi-\theta)}{\sqrt{1+[Q_{01}(\frac{\omega_{01}}{\omega}-\frac{\omega}{\omega_{01}})]^2}\sqrt{1+[Q_{02}(\frac{\omega_{02}}{\omega}-\frac{\omega}{\omega_{02}})]^2}}}$$

------ (13)

Where, ω_{01}, Q_{01}, D_1 and ω_{02}, Q_{02}, D_2 are frequency, Q factor and constant parameters for the two modes, respectively.

To describe the results, we employed an example here. There are two modes with the following parameters: $f_{01} = 825MHz$, $Q_{01} = 20000$, $D_1 = 0.01$ for mode 1 and $f_{02} = 825.1MHz$, $Q_{02} = 20000$, $D_2 = 0.02$, for mode 2, Fig. 6 shows the two separated modes as they should be.

The coupling coefficients D depend on the location of the probe corresponding to $\cos(\eta - \psi)$ and $\sin(\eta - \psi)$ allowing a wide range of values.

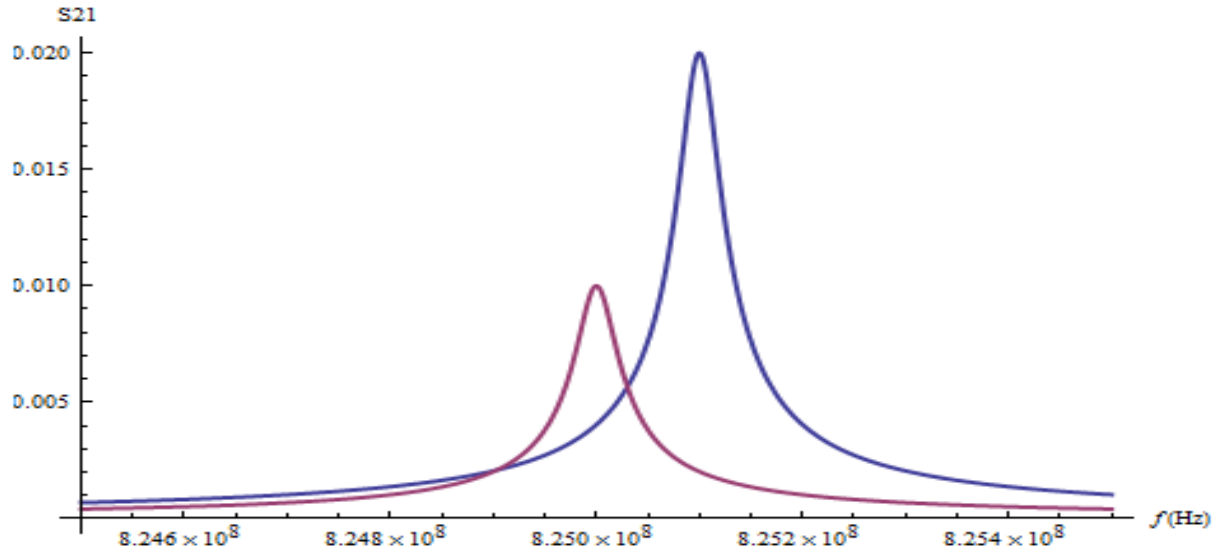

FIG. 9: Two separated modes

However, the network analyzer cannot see them separately as they are shown in Fig. 9. What it sees is the add-up result of the two modes and the results depend on the angle of the two vectors and coupling strength. The bandwidths of these two modes are distorted by each other and the *Q* values are different from what they should be. Fig. 10 shows the S_{21} of these two modes with different angles from 0 to π. And the *Q* values for different θs are listed in Table I. The two green curves are the original S21 curves without distortion. From both Table I and Figure 10, the bandwidths can be either wider or sharper than the original curve, which means the Q values can be either smaller or bigger than what it should be by 3dB method.

TABLE I. Q-Values

	Q_0	0	π/5	2π/5	3π/5	3.5π/5	4.5π/5	π
Mode1	20000	~	~	4852.9	19187	20625	27500	29464
Mode2	20000	18335	18752	19188	20627	21156	21713.2	21713

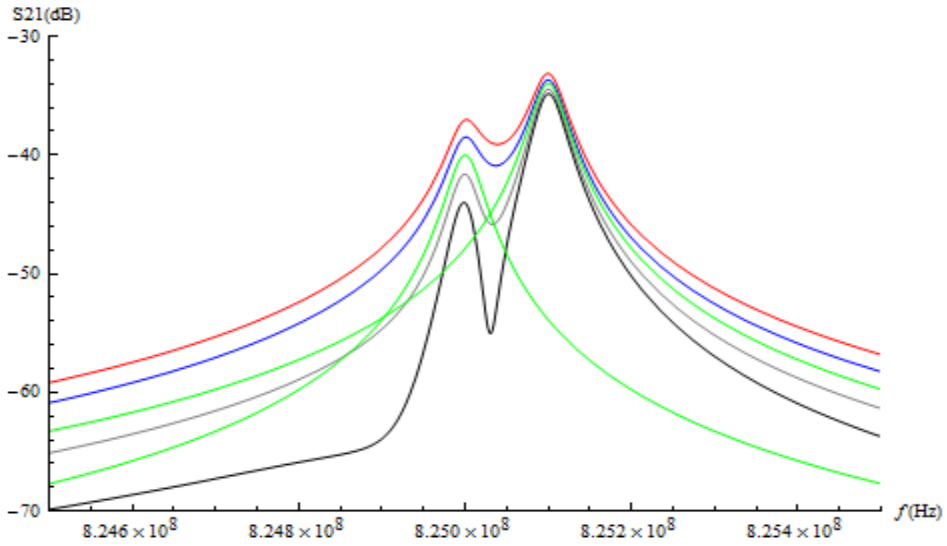

FIG. 10: S21of two splitting modes with different angle: 0 (Red), π/2 (Blue), 3.5π/5 (Gray), 4.5π/5 (Black) and two pure modes (Green)

IV. IMPROVEMENT OF Q-VALUE MEASUREMENT

As it is described in the above section, the *Q* values were distorted due to mode splitting, so to improve the measurement of the Q values, we should measure the S_{21} curve and fit the S_{21} with formula (13). We fitted all the dipole modes listed in the Section II with "Findfit" function in mathmetica. There are seven parameters: two Q-values, two frequencies, two coupling factors, and the phasor angle. From the measurement results, we can get the frequencies in small range. The amplitude of the S_{21} are determined by the coupling factor, thus the range for fitting is small as well. So basically, most of the effort is to find the Q-values and the phasor angle. The results

are shown in figure 11. It shows that the fitted Q values agree with the simulated results very well. Two typical fitting resulting is shown in figure 12.

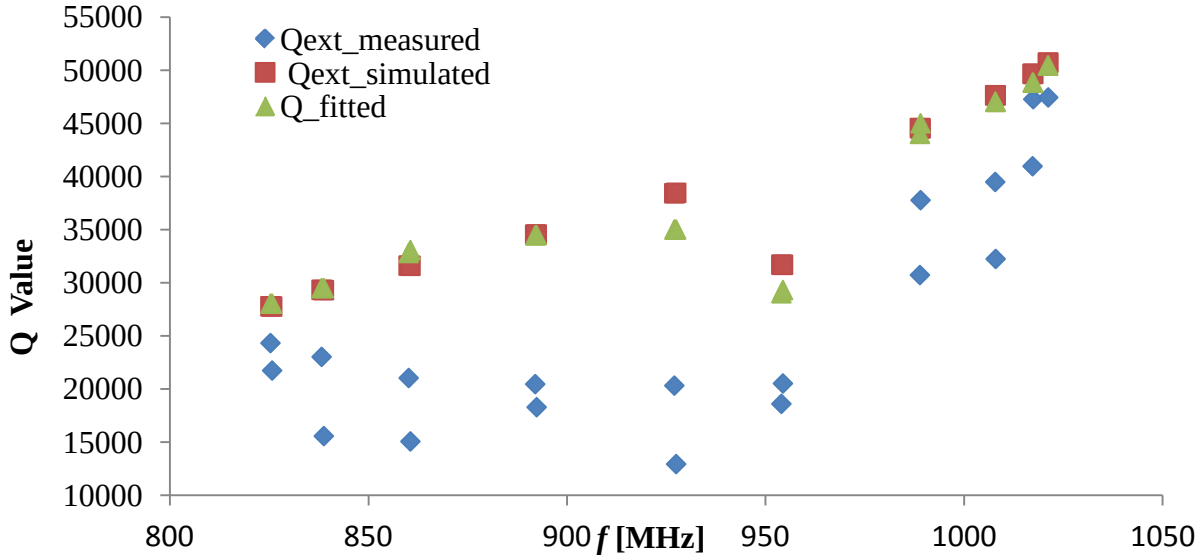

FIG.11: Comparison results from measurement, simulation and fitting results of BNL3 cavity

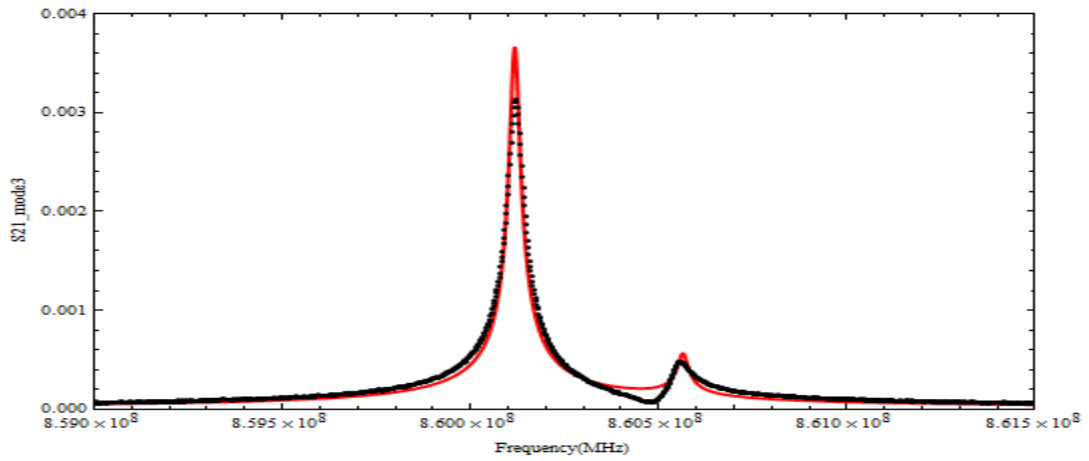

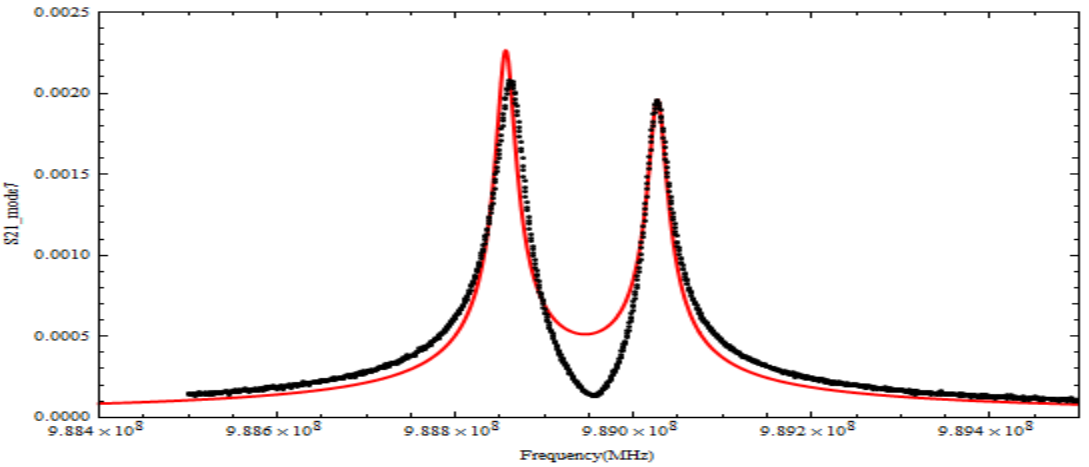

FIG. 12: S21 fitting results. Black dot: measured data; Red curve: fitting curve

V. SUMMARY

The measurement *Q* values at BNL3 copper prototype cavity are noticibly smaller than the simulation values. This paper discussed the conventional -3dB method of *Q* values measurement in the room temperature cavity and the issues of this method caused bythe field polarization of the slightlty elliptical cavity. The reasons of cavity polarization, which causes the S_{21} distortion, were described. The new S_{21} formula for the splitting modes was derived and used to fit the measurement data. The fitted S_{21} and *Q* values match the simulated results very well.

ACKNOWLEDGEMENTS

This work is supported by Brookhaven Science Associates, LLC under Contract No. DE-AC02-98CH10886 with the U.S. DOE, and Award No. DE-SC0002496 to Stony Brook University with the U.S. DOE. The authors would like to acknowledge Zenghai, Li, Lining Xiao, Kwok Ko and Ng Cho of SLAC for help with the Omega3P simulations.

REFERENCE

[1] Wencan Xu, I. Ben-Zvi, R. Calaga, H. Hahn, E. C. Johnson, J. Kewish, "High current cavity design at BNL," *Nucl. Instr. and Meth. A* **622** (2010) 17-20. Wencan Xu, etc. Design and RF measurements on the high-current 704 MHz superconducting RF cavity copper prototype at BNL, to be published.

[2] L.-Q. Lee, Z. Li, C. Ng, K. Ko, "Omega3P: A Parallel Finite-Element Eigenmode Analysis Code for Accelerator Cavities," SLAC-PUB-13529.

[3] Chu, Lan-Jen, "Electromagnetic Waves in Elliptic Hollow Pipes of Metal", J. Appl. Phys.9, 583 (1938);

[4] D. A. Goldberg, L. J. Laslett, R. A. Rimmer, "Modes of elliptical waveguide: a correction", LBL-28702.

[5] Jan G. Kretzschmar, "Wave propagation in hollow conducting elliptical waveguides", IEEE Transactions on microwave theory and techniques, P547-554, Sept. 1970.

[6] N. Marcuvitz, Waveguide Handbook, (Dover Publications, New York), p. 80